Face-centered-cubic to orthorhombic phase transition in single-crystal RbC_{60} analyzed by Raman scattering

J. Winter and H. Kuzmany

Universität Wien, Institut für Festkörperphysik, Strudlhofgasse 4, A-1090 Wien, Austria and Ludwig Boltzmann Institut für Festkörperphysik Wien, Kopernikusgasse, A-1060 Wien, Austria

(Received 23 February 1995)

Single crystals of C_{60} were doped with rubidium to the phase RbC_{60} by a load and equilibrate technique. No matter which nonequilibrium state of doping was reached, the equilibration procedure always resulted in the Rb monofulleride phase. Raman scattering for the fcc and for the orthorhombic phase is reported and compared with spectra of KC_{60}. For rapidly cooled crystals the latter are found to be identical with the spectra of the rubidium compound. A line at 344 cm^{-1} was found to be most characteristic for the orthorhombic phase in both cases and, together with some other new and very strong spectral features, considered as an indication of covalent bonds in a polymeric chain. The phase transition for the Rb phase was observed to start at 397 K on cooling with a hysteresis of about 17 K between the cooling and the heating cycle. The continuous shift of the pinch mode line during the process of the phase transition is considered as evidence for a growing linear chain during the process of the phase transition.

I. INTRODUCTION

Immediately after the discovery of metallic phases in charge transfer systems between C_{60} and alkali metals by Haddon *et al.*[1] a dramatic increase in the research activity on these systems started leading finally to a new class of materials with many interesting properties. Among others superconductivity was observed at rather high temperatures[2,3] for the systems A_3C_{60} with A one of the more bulky alkali metals. Following these discoveries a lot of attention was paid to more general systems with the composition A_xC_{60} where A is K, Rb, or Cs. x describes the stoichiometry of the composition and was found originally to obtain only the integer values 3, 4, or 6. These compounds may be assigned as classical alkali metal fullerides. In all of them the alkali metal donates its valence electron to the highest unoccupied t_{1u} level of the carbon molecule, rendering the latter in a charge state $-x$. Accordingly, in a simple one-electron picture all phases with x <6 should be metallic. In practice metallicity is only well established for the compounds with A= Rb or K and x=3.

More recently systems with $x = 1$ became attractive because of their unusual structural, magnetic, and electrical properties. These compounds were first observed from a Raman analysis of the potassium compound.[4] The existence of a high-temperature phase of KC_{60} was concluded from a characteristic downshift of the pinch mode frequency to 1460 cm^{-1} as compared to its value in a neutral fullerene molecule of 1467 cm^{-1} (at high temperatures). This phase turned out to be stable only above about 400 K and exhibited a segregation into uncharged and triply charged C_{60} below this temperature. This behavior was observed for thin C_{60} films as well as for single crystals[5] and confirmed by core level spectroscopy of the potassium 1s electrons.[6] From x-ray structural investigations the compound was found to have an fcc lattice with a rocksalt structure where the potassium ions are located on the octahedral interstitial lattice sites.[7]

Interestingly, the temperature dependence of the structural behavior was found to be different for the RbC_{60} system for which a room temperature stable phase was reported from IR spectroscopy on thin films, immediately after the discovery of the rocksalt phase for KC_{60}.[8,9] A NMR analysis for Rb and CsC_{60} revealed likewise a new phase at low temperatures with a broad resonance line for ^{13}C, ^{87}Rb, and ^{133}Cs.[10] The ^{13}C line was observed to be narrow in the high-temperature phase, indicating a quasifree rotation of the C_{60} ions. The angular correlation time was, however, found to be several orders of magnitude longer as compared to the neutral molecule at high temperatures. In a more detailed experiment a phase transition from fcc to an orthorhombic structure was found by Pekker *et al.*[11] at 410 K. This structure was suggested to consist of polymeric C_{60} chains where the individual cages were connected by a 2 + 2 cyclo addition along the face diagonal of the fcc unit cell. This polymerization process is stereochemically similar to the photopolymerization of C_{60} suggested by Rao *et al.*[12] Since the work of Pekker *et al.*[11] a lot of emphasis has been dedicated to the analysis of the nature of the orthorhombic state. Good evidence for its polymeric character was obtained from a detailed x-ray investigation which gave an unusual short C_{60}-C_{60} distance of 0.912 nm along the [110] direction of the original fcc lattice.[11] Even more, the bond lengths between the connected C_{60} molecules and also those of the neighboring carbon atoms revealed values consistent with a polymeric structure.[13] From an analysis of the temperature dependence of the electron-spin-resonance (ESR) line intensity the orthorhombic phase was suggested to be metallic at least between the fcc to orthorhombic phase transition and another transition to a spin density wave state

0163-1829/95/52(10)/7115(9)/$06.00

which was observed around 50 K.[14] CsC_{60} was found to behave similar to the Rb compounds in this point but KC_{60} was recently claimed to stay metallic down to very low temperatures.[15] From the NMR results the high-temperature phase was demonstrated to be paramagnetic whereas for the low-temperature phase the response from the metal spins indicate metallic behavior whereas the spins from the ^{13}C atoms indicate a nonmetal. This discrepancy between the behavior of the metallic spins and the carbon spins was claimed to be not necessarily an evidence against the metallicity of the polymer chains since a similar result is known for oxidic superconductors.[16]

The difference between the potassium system and the rubidium system with respect to the phase-separation was explained by the different size of the alkali atoms. The diffusion kinetics for the more bulky Rb atom is considered to be much slower so that a transition to the phase-separated state where alkali atoms have to change from the octahedral lattice site to the tetrahedral site is strongly suppressed. In some experiments it was observed that even for the potassium compound a phase separation was not observed but the transition occurred to the orthorhombic state as in the Rb system.[13,17] Most recently this was again studied in more detail and a new phase containing C_{60} dimers in a monoclinic crystal structure was found for KC_{60} after quenching from the fcc state.[18] Warming up of the compound from the quenched state was shown to lead to the orthorhombic phase.

Vibrational spectroscopy was expected to be a good check on the formation of the various phases in the AC_{60} systems. The transition to the orthorhombic phase was indeed observed by studying the IR reflectivity of RbC_{60} single crystals in a cooling experiment. A dramatic splitting of the threefold degenerate F_{1u} modes and a strong increase of the background reflectivity within a very narrow temperature range around 405 K characterized the transition.[19,20] A Raman investigation of the polymeric state was recently reported for very thin C_{60} films on a copper {111} substrate, intercalated to RbC_{60}.[21] Several strong new lines were observed, indicating a dramatic symmetry breaking of the C_{60} molecule as could be expected from a polymerization process.

We report in this paper a detailed Raman study of the high-temperature fcc phase and of the low-temperature orthorhombic phase for single crystal RbC_{60}, including the dynamics of the phase transition. As the most prominent result several new lines were identified as characteristic for the polymeric state and were compared to recent calculations.[22] From the behavior of these lines during the temperature cycle the phase transition was found to occur in a narrow temperature range of 15 K with a hysteresis between cooling and heating of 17 K. In addition most of the lines for the fivefold-degenerated H_g modes appear considerably splitted. Spectra obtained for rapidly cooled single crystals of KC_{60} were observed to be identical to those from the rubidium compound.

II. EXPERIMENT

The single crystals used were grown from highly purified C_{60} powder by the sublimation technique as described in Ref. 23. They had a smooth and shiny {100} face with typical dimensions of 1.5×2.5 mm. The crystals were mounted with silver paste on the sample holder of a cryostat to obtain a good thermal contact. Also two electrical contacts were fixed on the surface to get an additional control of the doping process. During this procedure the crystals were on air for about 2 h. Before the doping process was started the crystal was heated to 450 K for 12 h to outgas impurities like oxygen.

The cryostat was a slightly modified Haddon-type cell in which the doping process could be observed *in situ* in front of the Raman spectrometer. It allowed cooling and heating between room temperature and 480 K and also measurements at nearly liquid nitrogen temperature. The rubidium was approximately 35 cm away from the sample in a quartz tube and was heated from the outside. During the doping experiment the dynamical vacuum in the chamber was better than 10^{-4} Pa.

The doping process was performed at elevated temperature (> 400 K) and was controlled by *in situ* Raman measurements of the $A_g(2)$ pinch mode and the change of the resistance. The position of the pinch mode in the Raman spectrum is known to be very sensitive to the charge transfer from the rubidium atom to the fullerine. Because of the nearly linear shift of about 7 cm^{-1} per charge transfer, the mode is predestinate for the characterization of the doped state of the system.

Doping and controlling at high temperatures has the advantage that above 400 K no phototransformation occurs.[24] Accordingly the measured Raman spectra of the undoped and partially doped material were stable against irradiation with light. Thus, all changes in the Raman spectra originated from the doping process.

The doping of the sample was performed as a combination of a doping process in a temperature range between 400 K and 415 K and an equilibration process at a crystal temperature between 450 K and 475 K as described previously for IR experiments.[25] However, the Raman probe allows a much better control of this doping and equilibration cycles. Figure 1 illustrates this behavior. Spectrum (1) shows the $A_g(2)$ pinch mode of undoped C_{60} at 450 K, spectrum (2) the Raman response after 14 h doping with rubidium at a crystal temperature of 410 K. A small amount of Rb_3C_{60} (dashed arrow) can be observed together with some RbC_{60} (solid arrow) and a lot of undoped C_{60}. Heating the sample to 450 K [spectrum (3)] shows that the Rb_3C_{60} phase dissolves and more RbC_{60} is formed by diffusion of rubidium into the bulk. After a few cycles of this doping and equilibration process and at least about 40 h of doping a nearly homogeneous RbC_{60} fcc phase could be obtained up to the penetration depth of the green laser. This is demonstrated in Fig. 2 by comparing the response from an undoped material (dashed line) with the doped crystal at the same temperature. Note the remarkable weak Raman response of the $A_g(2)$ pinch mode in the RbC_{60} phase compared to undoped C_{60}. This repeated doping and equilibration process was found to work in general. At any state of the doping process the nonequilibrium phase ($x = 3, 6$) could be dissolved into the $x = 1$ compound on top of the undoped bulk of the crystal.

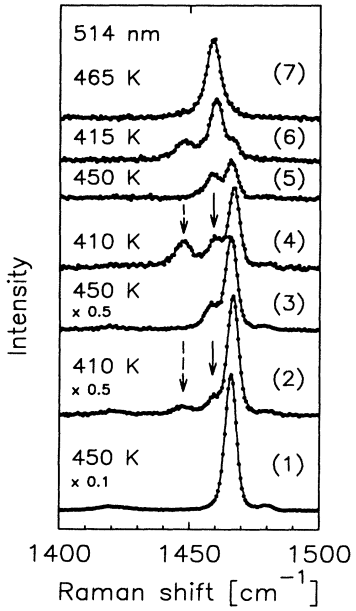

FIG. 1. Raman spectra between 1400 cm^{-1} and 1500 cm^{-1} during the doping and equilibration process. (1) undoped C_{60}; (2),(3) first doping-equilibration cycle; (4),(5) second doping-equilibration cycle; (6),(7) third doping-equilibration cycle.

For the excitation of the spectra an argon ion laser at 514.5 nm, a dye laser with Rhodamin 6G at 583 nm and 607 nm excitation, a HeNe laser at 633 nm and a pumped Ti-sapphire laser at 754 nm excitation were used. Various interference filters and a prism monochromator served to clean the excitation spectra from plasma lines. The laser light was focused to the sample with a diffraction limited spot size of about 30 μm. The laser intensities were limited to approximately 50 W/cm^2 (350 μW power). The scattered light was analyzed with a Dilor XY triple spectrometer in a backscattering geometry and detected by a nitrogen-cooled charge couple device detector. The Raman data were analyzed and fitted with Voigtian or Gaussian line shapes using a commercial computing program. All solid drawn lines shown in the figures of the experimental results are as obtained in this way. All linewidths are given as measured. The experimentally observed width of the laser line was 3 cm^{-1} in the case of the argon laser.

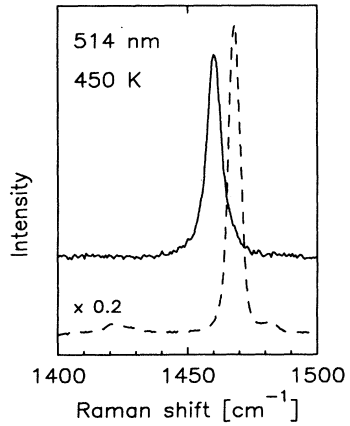

FIG. 2. Raman line for the pinch mode of a single crystal single phase RbC_{60} at 450 K (solid line) as compared to the line for the undoped material (dashed line) at the same temperature.

III. RESULTS

Experimental results of Raman spectra from RbC_{60} will be presented for various temperatures and as excited with various laser energies in comparison to spectra from undoped C_{60} crystals.

A. Raman spectra for the high-temperature and low-temperature phases

The spectra shown in Fig. 3 cover the whole frequency range of the fundamental molecular modes for various systems for comparison. Spectrum (a) is the well-known result for the undoped crystal with the dominating pinch mode line at 1467 cm^{-1} at 450 K. The other Raman-active H_g modes are indicated by the arrows and compiled in Table I. All frequencies in the table were obtained from a detailed line fitting procedure. Comparing the spectrum of Fig. 3(a) to the response of RbC_{60} at 450 K [Fig. 3(b)] the expected shift of the pinch mode by 7 cm^{-1} (as counted from its position at 450 K in the undoped phase) to 1460 cm^{-1} and a dramatic increase of the intensities for the modes $H_g(1)$ at 270 cm^{-1} and $A_g(1)$ at 497 cm^{-1} as compared to the intensity of the $A_g(2)$ mode is observed. A tentative assignment for the other H_g derived modes is again indicated by the arrows and correspondingly compiled in Table I, line RbC_{60}(HT). In contrast to the A_3C_{60} compounds even

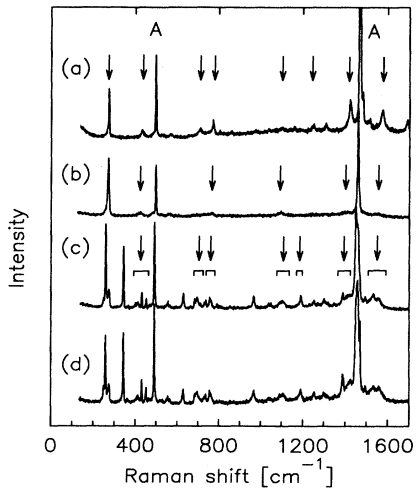

FIG. 3. Raman spectra of single crystal C_{60} compounds as excited with 514.5 nm, 300 μW. (a) neutral C_{60}, (b) RbC_{60} at 450 K, (c) RbC_{60} at room temperature, (d) KC_{60} at room temperature. The arrows and brackets indicate the positions of the H_g modes, the letter A those of the two A_g modes.

TABLE I. Positions of the Raman lines in undoped C_{60} and in fcc RbC_{60} at 450 K and in polymeric RbC_{60} at room temperature. Calculated values are from Adams *et al.* (Ref. 22). The assignment of the calculated frequencies to the fundamental modes is obtained by comparison with the experiment.

	$A_g(1)$	$A_g(2)$	$H_g(1)$	$H_g(2)$	$H_g(3)$	$H_g(4)$	$H_g(5)$	$H_g(6)$	$H_g(7)$	$H_g(8)$
C_{60}	495	1467	271	430	709	770	1099	1246	1421	1572
(HT)			266							
RbC_{60}	497	1460	270	421		766	1095		1406	1554
(HT)			263							
RbC_{60}	491	1460	248	402	684	731	1094	1190	1389	1530
(LT)		1450	259	412	695	738	1109	1251	1417	1559
			270	430	711	756				
			275	452		763				
			344[a]							
Calc.	461	1569	230	400	677	744	1030		1502	1616
			233	416	682	747	1074		1525	1625
			257	435	688	751	1088		1540	1632
			260		695				1549	
			330		698					

[a]The new line was tentatively listed in this column in order to compare it with the calculated values. It may not necessarily originate from the $H_g(1)$ mode but could be as well a new polymer mode.

the modes derived from $H_g(7)$ and $H_g(8)$ are observed, though strongly broadened and with a shift of 15 and 17 cm^{-1}, respectively. The large linewidth of 31 cm^{-1} for the $H_g(2)$ mode at 421 cm^{-1} is remarkable.

Cooling the crystal to room temperature with a moderate rate of about 5 K/min yields a basically different spectrum as shown in Fig. 3(c). The most dramatic difference is the appearance of a very strong new line at 344 cm^{-1}. In addition the lines derived from the H_g modes became well observable but strongly splitted as will be shown in detail below. Even the pinch mode shows two components. The arrows and brackets indicate a tentative assignment for the H_g-derived and A_g-derived modes. The spectrum shown here is very similar to the one reported by Lopinski *et al.* in Ref. 21. No significant new lines were observed below the $H_g(1)$ mode, at least not within the next lower 160 cm^{-1}. The last spectrum in Fig. 3 was obtained for KC_{60} cooled to room temperature with the same moderate cooling rate as for the Rb compound. The spectrum is more or less identical to the one obtained for the RbC_{60} and very different from the spectrum of a crystal which was equilibrated at high temperatures, just below the temperature for phase separation.[4,5] In the present case definitely no enhanced contribution to the spectrum from undoped C_{60} can be observed which would indicate a phase separation.

Details of the splitting for the most important regions of the spectrum are shown in Fig. 4 in a blowup form. The evaluated Raman line data are compiled in Table I, line RbC_{60}(LT). The details of the splitting are characteristically different for the various modes. Whereas the new line at 344 cm^{-1} does not split at all the $H_g(1)$ and $H_g(2)$ modes show a splitting into four components. Also, the two highest-frequency H_g modes split into at least two components.

The spectra show a dramatic sensitivity on the energy of the laser used for excitation. This is demonstrated for three regions of the vibrational spectrum in Fig. 5. The intensities as shown are not drawn to scale. As a matter of fact the Raman response decreases dramatically with decreasing laser energy used for the excitation and the doped part of the crystal becomes more and more transparent the longer the laser wavelength is. Finally, at 754 nm the spectrum from the RbC_{60} part of the crystal became unobservable. What remains to be seen is the rest of the underlying undoped part of the crystal which is still within the range of the penetration depth of the laser. The Raman lines of this part are marked by the arrow. The strong background in, e.g., part (c) of the figure originates from a luminescence which apparently

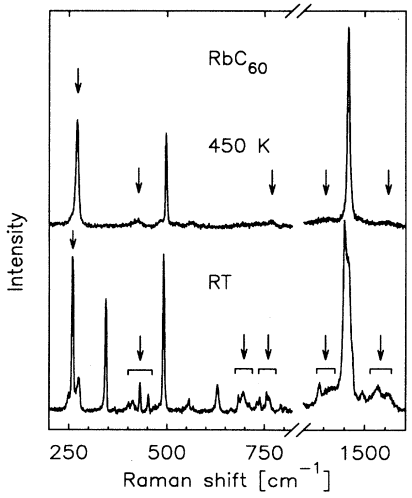

FIG. 4. Comparison of fundamental Raman modes for the high-temperature (top) and for the low-temperature (bottom) phase. The arrows and brackets indicate the positions of the H_g modes.

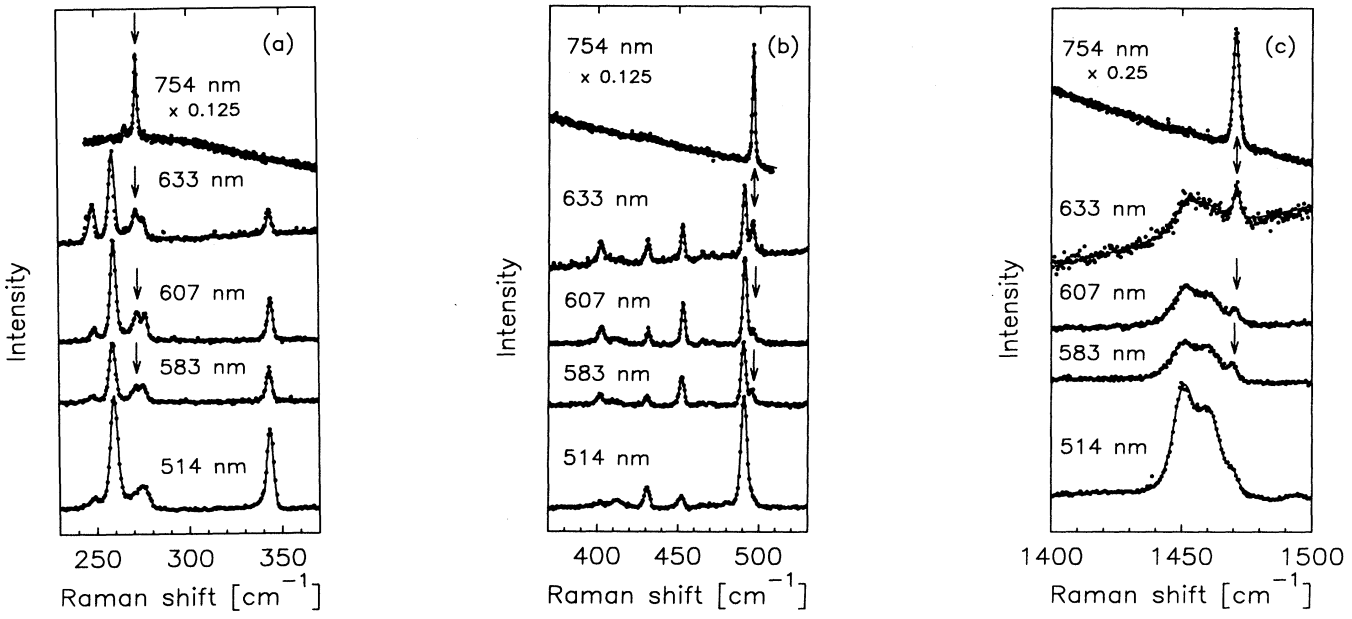

FIG. 5. Raman lines of RbC_{60} for three characteristic regions of the spectrum as excited with various laser lines indicated in the figure. Intensities for the various lasers are not drawn to scale. (a) Spectral range of $H_g(1)$ and the new mode at 344 cm^{-1}, (b) spectral range of $H_g(2)$ and $A_g(1)$, (c) spectral range of the $A_g(2)$ mode. The arrow indicates the contribution of the undoped material in the spectra.

has similar characteristics as in the undoped material or is in effect a luminescence from the underlying undoped part of the crystal.

B. Temperature dependence of Raman response

Figure 6 shows the Raman response for various selected regions of the spectrum during cooling through the phase transition and down to room temperature in detail. For each temperature the crystal was in a quasiequilibrium state. This is concluded from the stability of the Raman response for several hours at each temperature. Dramatic changes in the spectra are only observed in a very narrow temperature range from 397 K to 380 K. In part (a) of the figure the appearance of the new strong and unsplit

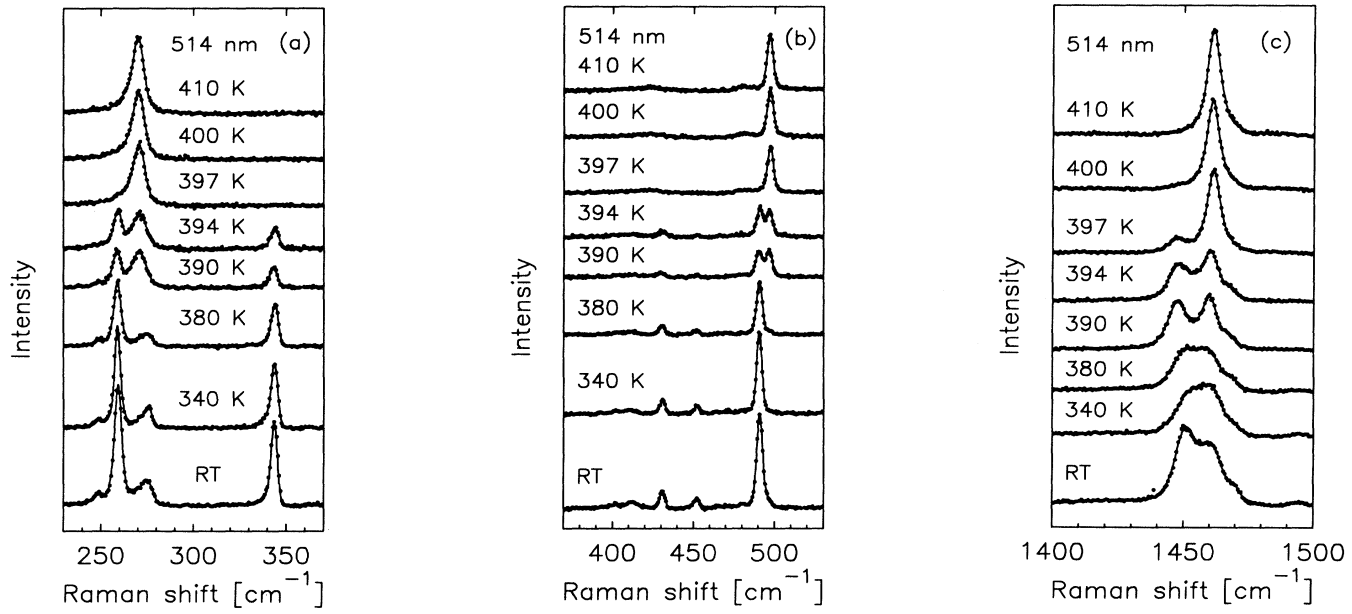

FIG. 6. Temperature dependence of the Raman response for various spectral regions. (a) $H_g(1)$ mode, (b) $A_g(1)$ mode, and (c) $A_g(2)$ mode. Intensities within one spectral range are drawn to scale.

line at 344 cm^{-1} at the phase transition is evident. It is important to note that this line was never observed for the photopolymerized material. Also the shift and the splitting of the $H_g(1)$ mode at the phase transition is evident. From part (b) the shift of the $A_g(1)$ mode is evident. The splitting seen for 394 K and 390 K originates from the simultaneous response of the two phases. In contrast, the splitting of the pinch mode shown in part (c) is intrinsic at any temperature below the phase transition.

Looking more carefully to the spectra, e.g., to those of Fig. 6(c), one gets the impression there could be an intermediate quasistable state between 394 K and 390 K before the two components of the lines nearly merge together. This impression is not really confirmed from a detailed analysis of the line shapes for the individual components as demonstrated in Fig. 7. Part (a) of the figure shows the parameters for the various components of the pinch mode. Solid circles refer to the mode in the high-temperature (HT) phase and to the high-frequency component of the low-temperature (LT) phase, open triangles to the low-frequency component in the orthorhombic phase, and open circles to a very small amount of undoped C_{60} observed from below the doped part of the crystal. The characteristic changes of the parameters between 380 K and 395 K indicate the temperature range where the phase transition occurs. The kink in the line position given by the solid circles in Fig. 7(a), top graph, confirms that the lines above 400 K and below 380 K are not the same. This becomes even more evident from the analysis of the intensities given below. The increase of the line position for the low-frequency component of the orthorhombic phase during the transition is noteworthy [top graph in Fig. 7(a), open triangles]. Similarly remarkable are the dramatic increases of the linewidths during the phase transition and their much larger value in the LT phase as compared to the fcc phase. So this line is obviously sensitive to the intermediate state of

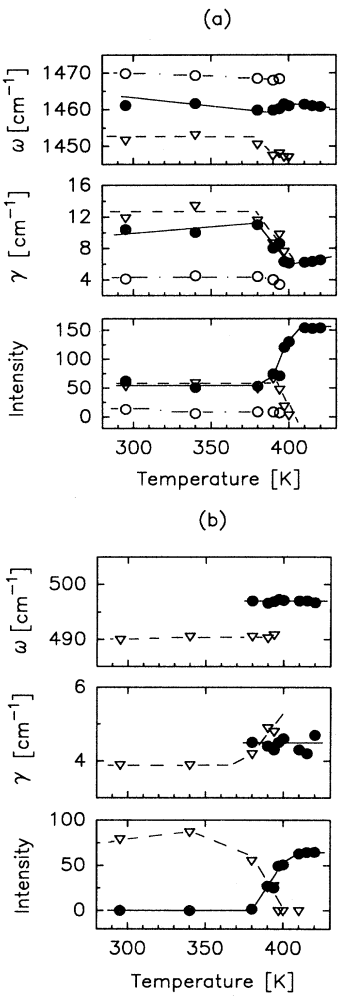

FIG. 7. Line shape parameters (position ω, width γ, intensity Int.) for selected Raman active modes versus temperature. (a) pinch mode, (b) $A_g(1)$. The symbols are as (•) RbC_{60} HT phase and LT phase, (▽) RbC_{60} LT phase, (○) C_{60}. The lines drawn are guides for the eye.

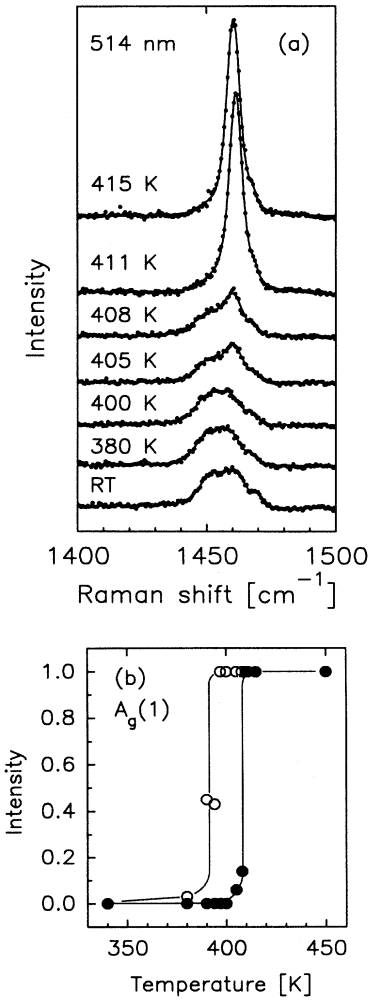

FIG. 8. Hysteresis of the phase transition as demonstrated for the pinch mode. (a) Spectra for increasing temperature for the pinch mode, (b) intensity for the $A_g(1)$ mode during a cooling and heating cycle. Intensities are normalized in the latter case to the begin and the end of the phase transition.

the phase transition. The behavior of line position and linewidths in the HT and LT equilibrium phases follow the expected trends, i.e., increasing and decreasing with decreasing temperature, respectively. The behavior of the intensities shown in the lowest part of the Fig. 7(a) is straightforwardly interpreted as the appearance of a new line at the phase transition (open triangles) and as the superposition of the disappearance of one line and the new appearance of a line at nearly the same position (solid circles).

The behavior for the $A_g(1)$ [Fig. 7(b)] derived mode is different. It appears at the phase transition without any change of line position and with a marginal decrease in linewidth. Consequently, this line is not sensitive to the intermediate state of the phase transition. Similarly, the most prominent line of the orthorhombic phase appearing at 344 cm^{-1} is insensitive to the intermediate state.

C. Hysteresis at the phase transition

Finally, the hysteresis of the phase transition was studied in more detail by warming up the crystal after it was slowly cooled to the LT phase. A series of spectra obtained for the pinch mode during a heating cycle is shown in Fig. 8(a). A similar result was obtained for the other characteristic modes. The temperature dependence of the intensities for the $A_g(1)$ mode is shown as an example for a full cooling and heating cycle in Fig. 8(b). The effective width of the hysteresis is about 17 K. The original spectrum of fcc RbC_{60} is completely restored at 411 K.

IV. DISCUSSION

The discussion of the experimental results as single-crystal single-phase RbC_{60} is justified in a sense that any contribution from undoped C_{60} to the spectra is of the order of 1% from its original value. This is so at least for excitation with the green laser and can be estimated from the very small contribution of the pinch mode for the undoped C_{60} as observed, e.g., in the spectra of Fig. 6. Even though the green laser does not penetrate the RbC_{60} part of the crystal the nature of the layered structure may lead to some residual stress in the doped part of the material. If so, the continuous character of the stress should rather cause a weak continuous broadening or shifting of the lines than a splitting. Thus, it is reasonable to anticipate that at least the observed splitting is intrinsic to the change in symmetry.

A. High-temperature phase

The Raman spectrum of the HT phase is as expected from previous results on the potassium compound.[5] This refers not only to the shift of the pinch mode by 7 cm^{-1} but also to the relative increase of scattering intensity for the modes $H_g(1)$ and $A_g(1)$ with respect to the pinch mode. Phase separation for the potassium compound was only obtained for an equilibration of the crystals just below the point of instability. Even relative low cooling rates across this point lead to the orthorhombic phase rather than phase separation. This confirms the suggestions that for potassium the diffusion kinetics at this point is faster than the kinetics of the displacive phase transition whereas the opposite holds for rubidium.

B. Low-temperature phase

The appearance of very strong new lines like the one at 344 cm^{-1} or the split pinch mode is a good indication for new covalent bonds and not just a symmetry breaking. It thus supports the establishment of a polymeric state in the orthorhombic phase in which all modes are nondegenerate. The factum that the splitting and the new line at 344 cm^{-1} are not observed in the photopolymer indicates some differences in the morphology of these two polymeric systems.[26]

It is interesting to compare the observed vibrational lines with spectra obtained recently from an *ab initio* calculation for the dimeric and for the polymeric system of C_{60} molecules,[22] even though in this work neutral dimers and neutral chains were studied. The results for the line positions and line splittings of the basic Raman active modes for the polymer are compiled in Table I (line calc.) according to this evaluation. The calculated splittings agree rather well with the experiment and even more, the strong new mode at 344 cm^{-1} is in very good agreement with the calculation. On the other hand the splitting of the pinch mode is obtained from the calculation only for the dimer. We may conclude, thus, that the chain length in the polymeric state is not very long even though at the present state of experiments and calculations a quantitative analysis is not yet possible.

The increasing transparency of the polymeric phase with decreasing laser energy as demonstrated in Fig. 5 is very likely due to the lack of absorption in the deep red spectral range as it is known for the classical alkali metal charge transfer systems A_3C_{60}, A_4C_{60}, and A_6C_{60}.[27] This gap in the absorption originates from the lack of allowed optical transitions from the bands such as the highest occupied molecular orbit (HOMO) in the original crystal (h_u symmetry) and below for wavelengths longer than 600 nm on the one side. The transitions from the partially filled t_{1u} band [the former lowest unoccupied molecular orbit (LUMO)] are on the other side not efficient for laser wavelengths shorter than 850 nm. This interpretation assumes that the electronic structure of the polymer phase is not characteristically different from the monomeric phase.

C. Phase transition

The hysteresis for the transition from the fcc to the orthorhombic phase indicates a first-order process. The intensities of the new lines, particularly those at 259 cm^{-1}, 344 cm^{-1}, 491 cm^{-1}, and 1450 cm^{-1}, represent the amount of material converted to the new phase. The shift in line position observed for the pinch mode during the phase transition indicates a growth of the chain length. This may be concluded from the fact that the

pinch mode is a vibration characterized by an oscillation of the bond length alternation. For such modes the relation between chain length and mode frequency is very well known from linear conjugated systems.[28,29] The dramatic increase of the linewidth by a factor of nearly 3 is consistent with this interpretation since during the phase transitions an increase in chain length as well as the creation of new chains can be expected which means a distribution of chain lengths is established. Since this behavior is only known for modes which exhibit a bond alternation, its absence for the other low-frequency modes is not surprising. If a model is accepted where the orthorhombic state is metallic, an additional contribution to the linewidth may originate from an interaction of the pinch mode with free carriers. At the present state of the experiments an significant contribution of this process to the linewidth can, however, not really be concluded.

V. CONCLUSIONS

Raman scattering was shown to be a very good technique to study the doping process of single-crystal C_{60} with alkali metals. Unless the crystal is fully doped always the phase AC_{60} is obtained if the system is equilibrated, at least for A = K, Rb. This holds provided the doping occurs above the temperature for phase transition or phase segregation. It means that at least for the high temperatures the phase AC_{60} has the lowest energy.

By cooling the AC_{60} crystals to room temperature even with a rather moderate speed a transition to a polymeric phase occurs for the two alkali-metal-doped systems studied. Phase separation for the potassium compound requires in general a long-time equilibration of the crystal at a critical temperature. This confirms the competing processes of segregation and polymerization. The exact conditions for the phase separation seem to vary with the character of the crystal. As a matter of fact they are not really well understood at present.

The process of the phase transition can be studied very well in both directions by following the change of characteristic Raman lines, the most prominent of which is observed at 344 cm^{-1}. The hysteresis indicates a first-order transition. The observed splitting of the degenerate modes is consistent with a complete loss of degeneracy in the low-temperature phase and agrees well with values calculated for a polymeric structure.

ACKNOWLEDGMENTS

We acknowledge M. Haluška for supporting us with the single crystals and the Hoechst AG for the C_{60} raw material. We are also grateful for valuable discussions with J.H. Weaver, D.M. Poirier, L. Forro, and L. Mihaly. The work was supported by the FFWF in Austria, Project No. P09741.

[1] R.C. Haddon A.F. Hebard, M.J. Rosseinsky, D.W. Murphy, S.J. Duclos, K.B. Lyons, B. Miller, J.M. Rosamilia, R.M. Fleming, A.R. Kortan, S.H. Glarum, A.V. Makhija, A.J. Muller, R.H. Eick, S.M. Zahurak, R. Tycko, G. Dabbagh, and F.A. Thiel, Nature **350**, 320 (1991).

[2] A.F. Hebard, M.J. Rosseinsky, R.C. Haddon, D.W. Murphy, S.H. Glarum, T.T.M. Palstra, A.P. Ramirez, and A.R. Kortan, Nature **350**, 600 (1991).

[3] M.J. Rosseinsky, A.P. Ramirez, S.H. Glarum, D.W. Murphy, R.C. Haddon, A.F. Hebard, T.T.M. Palstra, A.R. Kortan, S.M. Zahurak, and A.V. Makhija, Phys. Rev. Lett. **66**, 2830 (1991).

[4] J. Winter and H. Kuzmany, Solid State Commun. **84**, 935 (1992).

[5] J. Winter and H. Kuzmany, in *Proceedings of the International Winterschool on Electronic Properties of Novel Materials*, edited by H. Kuzmany, J. Fink, M. Mehring, and S. Roth (World Scientific, Singapore, 1994), p. 271.

[6] D.M. Poirier and J.H. Weaver, Phys. Rev. B **47**, 10 959 (1993).

[7] Q. Zhu, O. Zhu, N. Bykovetz, J.E. Fisher, A.R. McGhie, W.J. Romanow, C.L. Lin, R.M. Strongin, M.A. Cichy, and A.B. Smith III, Phys. Rev. B **47**, 13 948 (1993).

[8] T. Pichler and H. Kuzmany, in *Proceedings of the International Winterschool on Electronic Properties of Novel Materials,* edited by H. Kuzmany, J. Fink, M. Mehring, and S. Roth, Springer Series in Solid-State Sciences Vol. 117 (Springer-Verlag, Berlin, 1993), p. 281.

[9] D. Koller, M.C. Martin, and L. Mihaly, Mol. Cryst. Liq. Cryst. **256**, 275 (1994).

[10] R. Tycko, G. Dabbagh, D.W. Murphy, Q. Zhu, and J.E. Fischer, Phys. Rev. B **48**, 9097 (1993).

[11] S. Pekker, L. Forro, L. Mihaly, and A. Janossy, Solid State Commun. **90**, 349 (1994).

[12] A.M Rao, P. Zhou, K.-A. Wang, G.T. Hager, J.M. Holden, Y. Wang, W.-T. Lee, X.-X. Bi, P.C. Eklund, D.S. Cornett, M.A. Duncan, and I.J. Amster, Science **259**, 955 (1993).

[13] P. Stephens, G. Bortel, G. Faigel, M. Tegze, A. Janossy, S. Pekker, G. Oszlanyi, and L. Forro, Nature **370**, 636 (1994).

[14] O. Chauvet, G. Oszlanyi, L. Forro, P.W. Stephens, M. Tegze, G. Faigel, and A. Janossy, Phys. Rev. Lett. **72**, 2721 (1994).

[15] F. Bommeli, L. Degiorgi, P. Wachter, Ö. Legeza, A. Janossy, G. Oszlanyi, O. Chauvet, and L. Forro, Phys. Rev. B **51**, 20 (1995).

[16] R.E. Walstedt and W.W. Warren, Jr., Science **248**, 1082 (1990).

[17] S. Pekker, A. Janossy, L. Mihaly, O. Chauvet, M. Carrard, and L. Forro, Science **265**, 1077 (1994).

[18] Q. Zhu, D.E. Cox, and J.E. Fischer, Phys. Rev. B **51**, 3966 (1995).

[19] T. Pichler, R. Winkler, and H. Kuzmany, in *Proceedings of the International Winterschool on Electronic Properties of Novel Materials*, edited by H. Kuzmany, J. Fink, M. Mehring, and S. Roth (World Scientific, Singapore, 1994), p. 261.

[20] R. Winkler, T. Pichler, and H. Kuzmany, Appl. Phys. Lett. **66**, 1211 (1995).

[21] G.P. Lopinski, M.G. Mitch, J.R. Fox, and J.S. Lannin, Phys. Rev. B **50**, 16 098 (1994).

[22] G.B. Adams, J.B. Page, O.F. Sankey, and M. O'Keeffe, Phys. Rev. B **50**, 17 471 (1994).

[23] M. Haluška, H. Kuzmany, M. Vybornov, P. Rogl, and P. Fejdi, Appl. Phys. A **56**, 161 (1993).

[24] M. Matus, J. Winter, and H. Kuzmany, in *Proceedings of the International Winterschool on Electronic Properties of*

Novel Materials, Springer Series in Solid-State Sciences Vol. 117 (Springer-Verlag, Berlin, 1993), p. 255.
[25]T. Pichler, R. Winkler, and H. Kuzmany, Phys. Rev. B **49**, 15 879 (1994).
[26]J. Winter and H. Kuzmany (unpublished).
[27]T. Pichler, M. Matus, J. Kürti, and H. Kuzmany, Solid State Commun. **81**, 859 (1992).
[28]L. Salem, *The Molecular Orbital Theory of Conjugated Systems* (Benjamin, New York, 1974).
[29]H. Kuzmany, in *Frontiers of Polymer Research,* edited by P.N. Prasad and J.K. Nigam (Plenum, New York, 1991), p. 289.